

# Gap generation in topological insulator surface states by nonferromagnetic magnets

László Oroszlány<sup>1</sup> and Alberto Cortijo<sup>2</sup><sup>1</sup>*Department of Physics of Complex Systems, Eötvös University, H-1117 Budapest, Pázmány Péter sétány 1/A, Hungary*<sup>2</sup>*Instituto de Ciencia de Materiales de Madrid, CSIC, Cantoblanco, 28049 Madrid, Spain*

(Received 2 August 2012; published 26 November 2012)

Within a tight-binding approach, it is shown that, contrary to naive expectations, single-particle spectral gaps can be opened on the surface states of three-dimensional topological insulators by using commensurate out- and in-plane antiferromagnetic or ferrimagnetic insulating thin films.

DOI: [10.1103/PhysRevB.86.195427](https://doi.org/10.1103/PhysRevB.86.195427)

PACS number(s): 75.70.-i, 73.20.-r, 75.30.Gw, 85.75.-d

## I. INTRODUCTION

One of the most remarkable properties of a three-dimensional topological insulator is the presence of a topologically quantized magnetoelectric term (TMET) in its electromagnetic response. This term has far-reaching consequences since it constitutes a condensed-matter realization of axion electrodynamics.<sup>1,2</sup> Experimental signatures of the TMET include the quantized Kerr angle and Faraday rotation,<sup>3-5</sup> Casimir repulsion,<sup>6</sup> the inverse spin galvanic effect,<sup>7</sup> monopole images,<sup>8</sup> the surface half-integer Hall effect,<sup>9</sup> topological viscoelastic response,<sup>10</sup> just to name a few.

The key issue for the observability of the topologically quantized response is the breakdown of time-reversal symmetry in the surface of the otherwise time-reversal-invariant TI.<sup>9</sup> In terms of the electric and magnetic fields, the TMET is described by the effective action

$$S_\theta = \frac{\alpha}{4\pi^2} \int d^3\mathbf{r} dt \theta \mathbf{E} \cdot \mathbf{B}, \quad (1)$$

where  $\alpha$  is the fine-structure constant and  $\theta$  is the so called axion parameter which takes the value of 0 or  $(2n+1)\pi$  with  $n \in \mathbb{N}$  in trivial and topological insulators, respectively.<sup>9</sup> Alternatively, when a TI/trivial insulator interface is considered, one can understand the TMET as a Chern-Simons (CS) term induced in the electromagnetic response of the insulator by the gapped surface states of a TI that are described by the usual massive Dirac Hamiltonian:<sup>9,11</sup>

$$H_D = v(\boldsymbol{\sigma} \times \mathbf{k}) \cdot \hat{\mathbf{z}} + m\sigma_z, \quad (2)$$

where  $v$  is the Fermi velocity and  $m$  is the induced mass of the Dirac states. In this case, the value  $\theta = \pi$  corresponds to the value  $\sigma = \frac{1}{2}\text{sgn}(m)$  for the Hall coefficient in the corresponding CS term. In short, breaking time-reversal symmetry opens a gap in the TI surface states, thus making the TMET observable.<sup>11</sup>

The main message of this work is that a more general class of magnetic materials can also be used to control the electronic gap of the surface states. We argue that antiferromagnetic and ferrimagnetic materials can, in principle, be considered as gap generators, and that contrary to common belief, and as shown by Fu,<sup>12</sup> an in-plane magnetic configuration can also open gaps, as depicted in Fig. 1.

Within the effective low-energy approximation described by (2), there are several proposals in the literature for opening a gap in the helical metal by means of weak magnetic fields through a Zeeman term,  $H_Z = g\mu_B \boldsymbol{\sigma} \cdot \mathbf{B}$ ,<sup>13</sup> or through

exchange coupling to ferromagnetic thin films,  $H_{\text{exc}} = J\mathbf{M} \cdot \boldsymbol{\sigma}$ ,<sup>9</sup> and magnetic impurities,  $H_{\text{imp}} = J \sum_j \mathbf{S}_j \cdot \boldsymbol{\sigma} \delta(\mathbf{r} - \mathbf{R}_j)$ .<sup>14-16</sup> The exchange coupling between magnetic thin films and TI is the most appealing one from a theoretical point of view because it not only provides a simple mechanism to develop the theory of the TMET, but it allows us to look for unexpected effects that can alter the thin-film magnetization dynamics.<sup>7,17</sup> However, this proposal is experimentally challenging, and it also poses some questions. First of all, it is not so easy to find insulating ferromagnetic materials. Some candidate materials such as GdN and EuO have been theoretically suggested,<sup>3,7</sup> but to the best of our knowledge so far there is no experimental evidence supporting this claim. Also, even if ferromagnetic insulating thin films were available, it is not guaranteed that the thin-film magnetization would point in the out-of-plane direction.<sup>18</sup> There is the problem of a possible relative displacement between the TI surface lattice structure and the thin-film lattice structure and even the issue of the two lattices not being commensurate. These problems are at the heart of the experimental difficulties for implementing this mechanism.

Directly using Eq. (2) implicitly forces us to consider a continuum medium approach for the magnetization.<sup>19</sup> The question is then how to construct an effective description of the exchange coupling between the surface electronic spin and the magnetization starting from a microscopic model. For ideal insulating ferromagnets, the most naive way would be to couple the electron spin with the averaged magnetization in the magnetic unit cell. However, when more realistic magnetic insulators are considered, we immediately run into difficulties. For instance, this approach automatically rules out the possibility of considering antiferromagnetic insulators as magnetic material candidates. Also, it is not at all clear what the correct form for a continuum description of the magnetization of a ferrimagnetic insulator is. Motivated by these experimental and theoretical issues, we address in this work the problem of coupling a magnetically active thin film to the surface electronic states of a TI employing a tight-binding approach.

The rest of the paper is organized as follows: In Sec. II, the tight-binding model for the system formed by a TI and a magnetic layer is described. In Sec. III, we describe the results obtained by solving the tight-binding model for both out-of-plane and in-plane magnetic configurations, while in Sec. IV we analyze some magnetic materials as tentative candidates for experimentally testing the results presented herein. In Sec. V, we review and briefly comment on our findings.

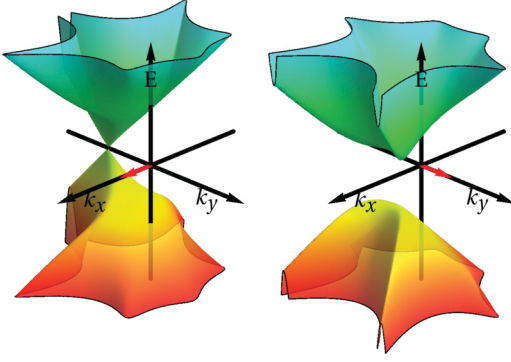


FIG. 1. (Color online) Low-energy spectrum of the surface states of a TI in homogeneous in-plane magnetization. Red arrows show the direction of the magnetization field.

## II. THE MODEL

To study qualitatively the ways in which the gap can be microscopically induced in the surface spectrum, we will employ a tight-binding model valid for the topological insulators of the  $\text{Bi}_2\text{X}_3$  family, which include the prototypical examples of TIs  $\text{Bi}_2\text{Se}_3$  and  $\text{Bi}_2\text{Te}_3$ . We will then follow Refs. 20 and 21 and consider a  $\text{Bi}_2\text{Se}_3$  sample made of  $N$  quintuple layers (QLs) grown in the (111) direction and terminated in Se planes. The surface will thus have a triangular lattice structure. We are interested in the band structure around the Fermi level, so the tight-binding basis set will be made of linear combinations of the atomic orbitals ( $|p_{\text{Bi}}^+, \uparrow\rangle, |p_{\text{Se}}^-, \uparrow\rangle, |p_{\text{Bi}}^+, \downarrow\rangle, |p_{\text{Se}}^-, \downarrow\rangle$ ). The superscript reflects the parity of the state, and the second index is the spin polarization. The tight-binding Hamiltonian in real space can be written in this basis in the following way:<sup>20,21</sup>

$$H = \sum_{\mathbf{n}} C_{\mathbf{n}}^\dagger \hat{\epsilon} C_{\mathbf{n}} + \sum_{\mathbf{n}, \mathbf{a}_i/\mathbf{b}_i} C_{\mathbf{n}}^\dagger \hat{t}_{\mathbf{a}_i/\mathbf{b}_i} C_{\mathbf{n}+\mathbf{a}_i/\mathbf{b}_i} + \text{H.c.} \quad (3)$$

Here the lattice vectors  $\mathbf{a}_i$  and  $\mathbf{b}_i$  connect unit-cell positions within the same QL and of different QLs, respectively, and  $\mathbf{n}$  labels the lattice positions as defined in Refs. 20 and 21. We use  $a = |\mathbf{a}_i|$  as the lateral spatial length scale. The on-site energy  $\hat{\epsilon}$  and hopping terms  $\hat{t}_{\mathbf{a}_i/\mathbf{b}_i}$  are  $4 \times 4$  matrices that can be written as a linear combination of  $\Gamma_i$  matrices, which are matrix products of spin  $\sigma$  and parity  $\tau$  Pauli matrices:

$$\begin{aligned} \hat{\epsilon} &= \epsilon_0 \Gamma_0 + m \Gamma_5, \\ \hat{t}_{\mathbf{a}_1} &= A_0 \Gamma_0 - i(A_{12} \Gamma_3 - A_{14} \Gamma_2) + A_{11} \Gamma_5, \\ \hat{t}_{\mathbf{b}_1} &= B_0 \Gamma_0 + i(B_{12} \Gamma_4 - B_{14} \Gamma_1) + B_{11} \Gamma_5, \\ \Gamma_{1,2} &= \tau_1 \otimes \sigma_{1,2}, \quad \Gamma_3 = \tau_1 \otimes \sigma_3, \\ \Gamma_{4,5} &= \tau_{2,3} \otimes \sigma_0, \quad \Gamma_0 = \tau_0 \otimes \sigma_0, \end{aligned} \quad (4)$$

with  $\sigma_0$  and  $\tau_0$  being the identity matrix. The remaining hopping matrices  $\hat{t}_{\mathbf{a}_{2,3}/\mathbf{b}_{2,3}}$  can be obtained from (4) by applying the rotation operation  $R_3 = \exp(i\frac{\pi}{3}\sigma_3 \otimes \tau_0)$ . The Hamiltonian (3) is thus made of intra-QL hopping terms and on-site energies and hopping terms coupling different QLs. In all calculations presented here, we use  $B_{11} = 1$ ,  $A_{14} = 1.4$ ,  $A_{12} = B_{12} = 3$ ,  $A_{11} = 2$ ,  $m = -10$ , and  $B_{14} = A_0 = B_0 = 0$  for modeling a bulk TI.<sup>21</sup> Next we add an exchange term coupling to the Se

atomic orbitals in (3) of the first QL of the form

$$H_{\text{exc}} = J \sum_{\mathbf{n}} \mathbf{S}(\mathbf{R}_{\mathbf{n}}) C_{\mathbf{n}}^\dagger \Sigma C_{\mathbf{n}}. \quad (5)$$

The matrices  $\Sigma$  are of the form  $\Sigma = \frac{1}{2}(\tau_0 - \tau_3) \otimes \sigma$  and now  $\mathbf{R}_{\mathbf{n}}$  represents the lattice positions of the Se atoms in the outer part of the first QL. The important observation here is that the magnetic and surface lattices *do not need to be the same for generic magnetic layers* so the magnetic moment of the magnetic layer  $\mathbf{S}(\mathbf{R}_{\mathbf{n}})$  at  $\mathbf{R}_{\mathbf{n}}$  will not be the magnetic moment of each magnetic position. Usually the magnetic moments represent the magnetic moment associated with a bounded atomic orbital with a short spatial extension, so not all the magnetic moments will couple in the same manner to the electronic spins on the surface, and the coupling will be stronger for nearer atoms. The two previous observations lead us to define  $\mathbf{S}(\mathbf{R}_{\mathbf{n}})$  as

$$\mathbf{S}_{\text{eff}}(\mathbf{R}_{\mathbf{n}}) \equiv \sum_i \mathbf{S}(\hat{\mathbf{R}}_i) \Phi(\mathbf{R}_{\mathbf{n}} - \hat{\mathbf{R}}_i), \quad (6)$$

where now the sum is performed over the magnetic lattice positions. The function  $\Phi$  encodes the information about the short-range character of the localized magnetic orbitals. In our calculations, we have chosen a Gaussian profile,  $\Phi(\mathbf{r}) = e^{-r^2/\beta}$ , parametrized by the parameter  $\beta$  which has the meaning of the (squared) mean size of the spatial profile of the magnetic orbital. We have checked that any other choice for  $\Phi$  does not modify the qualitative results presented in this work. It is important to note that for a given Se position, nearby moments will contribute to  $\mathbf{S}(\mathbf{R}_{\mathbf{n}})$  but not equally if there is a relative displacement between the two sublattices. This key observation is interesting because it opens the possibility of considering not just ferromagnetic, but also other types of magnetic ordering as a candidate for inducing gaps in the TI surface states by the exchange coupling mechanism.

## III. RESULTS

To show the ideas explained above at work, let us consider first the case in which the initial positions of the magnetic lattice lie in the middle of the triangles formed by the surface lattice, as is shown in Fig. 2(c), and calculate the spectrum with Eqs. (3)–(6). Consider now a relative in-plane displacement between the lattices by moving the magnetic bipartite lattice a distance  $\delta y$  with respect to the center of the triangle in the  $OY$  direction. We shall investigate the three cases of ferromagnetic ( $\mathbf{S}_1 = \mathbf{S}_2$ ), antiferromagnetic ( $\mathbf{S}_1 = -\mathbf{S}_2$ ), and ferrimagnetic ( $\mathbf{S}_1 = -5\mathbf{S}_2$ ) out-of-plane configurations. To compare our tight-binding results with the mass parameter  $m$  defined in Eq. (2), we show in Fig. 2(a) the value of the gap defined as  $m = |\min[E_c(\mathbf{k})] - \max[E_v(\mathbf{k})]|/2$ , where  $E_c(\mathbf{k})$  and  $E_v(\mathbf{k})$  are the lowest conduction and highest valence bands, respectively. For the ferromagnetic case, the system always develops a nonzero gap, as expected, irrespective of the relative position of the two lattice sites. The modulation in the value of the gap is understood in terms of the different contribution of the magnetic moments to  $\mathbf{S}_{\text{eff}}(\mathbf{R}_j)$ . Much more interesting are the cases of ferrimagnetic and antiferromagnetic lattice structures. The first important observation is that in both cases, a gap is opened when varying the relative position

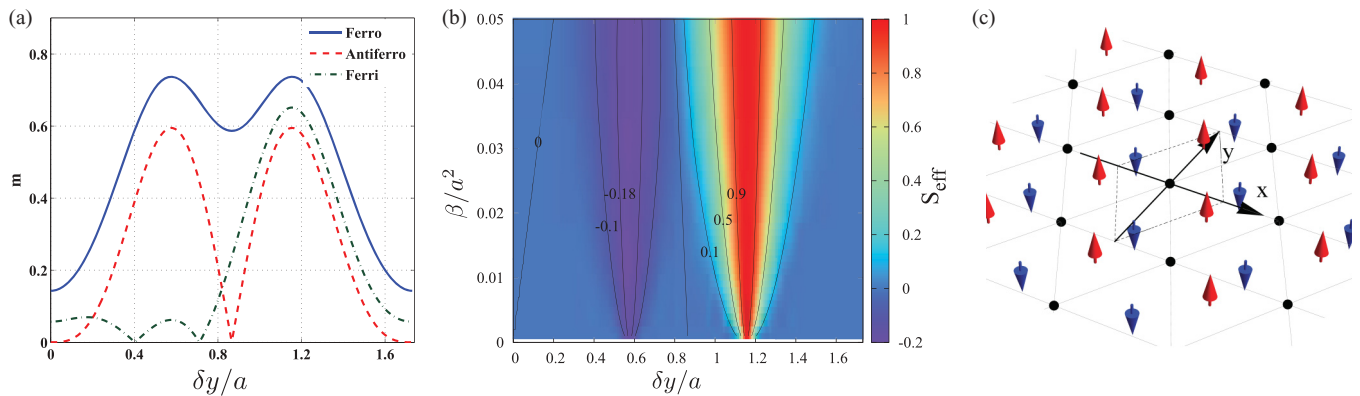


FIG. 2. (Color online) (a) Exchange-induced gap  $m$  (in units of  $B_{11}$ ) on the TI surface states vs the relative in-plane displacement  $\delta y$ . Blue (solid), red (dashed), and green (dashed-dotted) lines correspond to ferromagnetic, antiferromagnetic, and ferrimagnetic lattices, respectively. For the ferrimagnetic configuration,  $\mathbf{S}_1 = -5\mathbf{S}_2$  and  $\beta = 0.02a^2$ . (b) The effective Zeeman field on the surface as a function of the relative displacement  $\delta y$  between the magnetic and the TI lattices and the localization parameter  $\beta$ . (c) Real-space configurations for the TI surface. Black dots represent lattice Se positions and the arrows correspond to a hexagonal antiferromagnetic lattice.

of the lattices, showing that in principle one can open gaps in the TI surface states by the interaction with ferri- and antiferromagnetic layers. In principle, nothing guarantees that the magnetic lattice sites must lie on the exact center of the triangles formed by the surface positions, but the gap might be still open. Moreover, if during the fabrication process it were possible to control the relative in-plane displacement, the gap could be tuned. Another important observation is that although  $m$  is a positive-definite quantity by construction, the value of the effective Zeeman coupling is not. Indeed it will change its sign, as is shown in Fig. 2(b), where the effective Zeeman term is plotted as a function of the lattice displacement  $\delta y$  and the value of  $\beta$ . This change of sign of the Zeeman coupling due to the change in the relative displacement between lattices is a signature of a topological phase transition in the case of ferrimagnets, and this is also true for generic antiferromagnetic configurations. As can be readily seen in Fig. 2(b), there is always a change of sign of  $\mathbf{S}_{\text{eff}}$  irrespective of how tight the magnetic atomic orbitals are to their lattice sites.

So far, we have considered magnetic configurations in thin layers with the magnetization being out-of-plane. It is well known that when thin-film geometries are considered for ferromagnets, it is more energetically favorable for the system to have the magnetization in-plane.<sup>18,22</sup> From the form of (2), an in-plane homogeneous magnetization would not induce any gap since an in-plane magnetic moment would just shift the position of the Dirac point. Actually this is not the case, and a gap can be induced when lattice effects are considered in addition to (2), as was shown by Fu.<sup>12</sup> We can add to (2) the two next-to-leading terms in the expansion in momenta:<sup>12</sup>

$$H_w = \frac{\mathbf{k}^2}{2m_0}\sigma_0 + \alpha\mathbf{k}^2(\boldsymbol{\sigma} \times \mathbf{k}) \cdot \hat{\mathbf{z}} + \lambda(k_x^3 - 3k_xk_y^2)\sigma_z, \quad (7)$$

where  $m_0$ ,  $\alpha$ , and  $\lambda$  come from the comparison between tight-binding band-structure calculations and ARPES measurements.<sup>23</sup> When the Hamiltonian  $H_D + H_w$  is considered together with  $H_{\text{exc}} = J_{\parallel}\boldsymbol{\sigma}_{\parallel}\mathbf{m}_{\parallel}$ , it is apparent that a gap of value  $\tilde{m} = \lambda \frac{J_{\parallel}}{v^3}(m_y^3 - 3m_y m_x^2)$  appears at  $\mathbf{k}_g = \frac{J_{\parallel}}{v}\mathbf{m}_{\parallel} \times \hat{\mathbf{z}}$ , as is shown in Fig. 1. Note that the gap is zero for moments

pointing in the  $x$  direction and is maximal for the  $y$  direction, and it has an overall sixfold rotational symmetry. Apart from the mass generation due to the hexagonal terms, there is a self-doping effect defined through the parameter  $\mu = |\min[E_c(\mathbf{k})] + \max[E_v(\mathbf{k})]|/2$  due to the first term in (7). The effective model  $H_D + H_w + H_{\text{exc}}$  can be considered to be a good description for the interaction between the TI surface states and smooth varying ferromagnetic in-plane magnetization. However, as we argued before, there are many materials for which the magnetization varies at the order of the lattice spacing and the above effective description cannot be directly applied. Even in such cases, a nonvanishing gap can be found if one goes to the microscopic description of the system.

We will exemplify this situation considering the kagome lattice with classical planar magnetic configurations. The magnetism on this frustrated lattice is a current subject of research.<sup>24</sup> In particular, we have chosen the  $q=0$  and  $q=\sqrt{3} \times \sqrt{3}$  ground-state spin configurations as plotted in the insets of Fig. 3. To monitor the evolution of the spectral properties of the system, we have chosen the lateral displacement  $\delta x$  between lattices in the  $OX$  direction as a control parameter. In this way, the magnetic moment sitting on the horizontal axis will play a dominant role. The results for the gap and for the self-doping are also displayed in Fig. 3. We can easily understand the results by keeping in mind that the exchange interaction between magnetic moments and electron spins is short-ranged, and by recalling the behavior of the gap with the magnetic moment components according to Fu's model, as we argued below Eq. (7). In the inset of Fig. 3(a), the red sublattice magnetization points along the  $OY$  direction, so the gap will open when this sublattice magnetization is closest to the atomic lattice. In contrast, in the inset of Fig. 3(b) the red sublattice magnetization points along the  $OX$  axis, so according to Fu's model, no gap will be generated. Also, it is expected that both configurations will give rise to a nonvanishing self-doping effect (the shift of the energy of the Dirac point) when the effective magnetization is nonzero, as is shown in Fig. 3(b). Another important observation is that different in-plane magnetic configurations in adjacent space regions

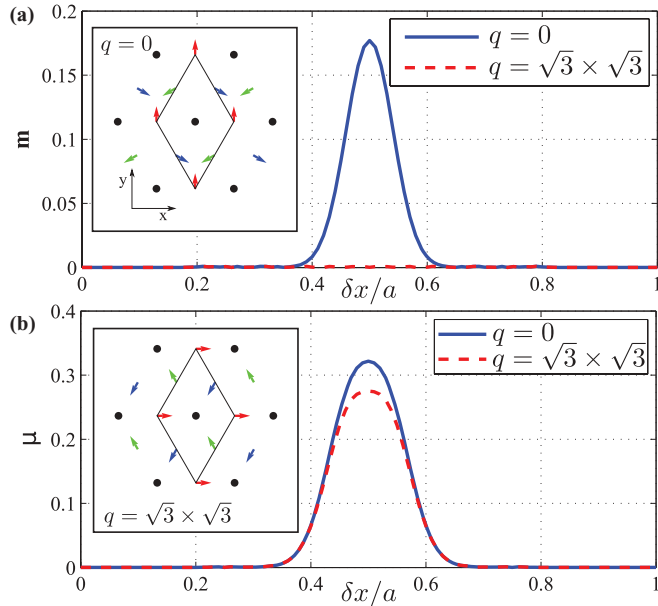


FIG. 3. (Color online) Evolution of the gap (a) and the self-doping (b) as a function of the relative in-plane displacement  $\delta\mathbf{x}$  between the two sublattices, as is explained in the text. Insets correspond to magnetic configurations with  $\delta\mathbf{x} = 0$ .

(Néel domain walls<sup>25</sup>) might induce a mass with opposite sign which would generate chiral 1D fermionic states.<sup>12</sup>

#### IV. EXPERIMENTAL FEASIBILITY

One of the proposed ferromagnetic insulators is  $\text{EuO}$ .<sup>26</sup> It possesses a gap of the order of 1.2 eV and it crystallizes in the simple cubic structure, not commensurate to the triangular lattice structure of the surface, introducing further complexity in the problem. In contrast to ferromagnetic insulators, ferrimagnetic insulators offer more reliable experimental opportunities. The ferrimagnetic insulating state is present in nature in many compounds and in many crystalline structures, and ferrimagnetic thin films can be manufactured in many ways.<sup>27</sup> Among them, we highlight the hexagonal ferrites of which  $\text{PbFe}_{12}\text{O}_{19}$  is the archetypal material. They crystallize in the hexagonal magnetoplumbite structure having a rather complex atomic configuration. Many other ferrites grow in the spinel structure, such as the magnetites ( $\text{Fe}_3\text{O}_4$ ) and cobalt ferrites ( $\text{CoFe}_2\text{O}_4$ ) that might be grown in thin

films with appreciable out-of-plane magnetization.<sup>28</sup> Although  $\text{CoFe}_2\text{O}_4$  has a strong relative in-plane displacement between the magnetic and the Se lattice structure and the results presented here are not directly applicable, we suggest it as prospective candidate for experimentally analyzing the effect of ferrimagnetism on the surface states of a TI. Concerning in-plane magnetic configurations, we can mention kagome systems with different planar spin ground states such as  $\text{SrCr}_9\text{Ga}_3\text{O}_{19}$ , herbertsmithite, jarosite, and many others.<sup>29</sup>

#### V. CONCLUSIONS

In the present paper, we have addressed the question of whether the effective Hamiltonian (2) is valid when the helical surface states of a TI are coupled to magnetically active layers. By using a tight-binding model for both the TI and the magnetization, we have shown that contrary to the (perhaps too) naive expectation that the helical spin couples to the total magnetization present in the unit cell, it couples to a *weighted average* of the magnetic moments present in the unit cell. This result tells us that, in principle, there is no physical reason for ruling out antiferromagnetic insulating thin films as candidates for inducing gaps in TI surface states. We have considered also the possibility of ferrimagnetic insulating thin films. In all the cases, we have shown that the magnetic exchange mechanism induces a gap in these surface states. As a result, we have found that the gap is sensitive to the relative displacement between the magnetic and surface lattices. We have considered also the realistic situation in which the film magnetization is in-plane and homogeneous. In this case, a gap might be opened due to hexagonal warping effects<sup>12</sup> even for materials whose thin-film magnetization is textured at the scale of the lattice spacing, inducing a zero average magnetic moment per unit cell.

#### ACKNOWLEDGMENTS

The authors gratefully acknowledge Carlos Pecharromán, András Pályi, József Cserti, and M. A. H. Vozmediano for valuable comments and suggestions. A.C. acknowledges the CSIC JAE-doc fellowship program and the Spanish MEC through Grants No. FIS2011-23713 and No. PIB2010BZ-00512 for financial support. O.L. acknowledges the support of the Hungarian OTKA (K81492, K76010, K75529, NK72916, NNF78842), and TAMOP (-4.2.1/B-09/1/KMR-2010-0002, -4.2.1/B-09/1/KMR-2010-0003) grants and the EU grant NanoCTM.

<sup>1</sup>F. Wilczek, *Phys. Rev. Lett.* **58**, 1799 (1987).

<sup>2</sup>A. Karch, *Phys. Rev. Lett.* **103**, 171601 (2009).

<sup>3</sup>W.-K. Tse and A. H. MacDonald, *Phys. Rev. Lett.* **105**, 057401 (2010).

<sup>4</sup>J. Maciejko, X. L. Qi, H. D. Drew, and S. C. Zhang, *Phys. Rev. Lett.* **105**, 166803 (2010).

<sup>5</sup>G. S. Jenkins, A. B. Sushkov, D. C. Schmadel, N. P. Butch, P. Syers, J. Paglione, and H. D. Drew, *Phys. Rev. B* **82**, 125120 (2010).

<sup>6</sup>A. G. Grushin and A. Cortijo, *Phys. Rev. Lett.* **106**, 020403 (2011).

<sup>7</sup>I. Garate and M. Franz, *Phys. Rev. Lett.* **104**, 146802 (2010).

<sup>8</sup>X. L. Qi, R. Li, J. Zang, and S. C. Zhang, *Science* **323**, 1184 (2009).

<sup>9</sup>X.-L. Qi, T. L. Hughes, and S.-C. Zhang, *Phys. Rev. B* **78**, 195424 (2008).

<sup>10</sup>T. L. Hughes, R. G. Leigh, and E. Fradkin, *Phys. Rev. Lett.* **107**, 075502 (2011).

<sup>11</sup>X. L. Qi and S. C. Zhang, *Rev. Mod. Phys.* **83**, 1057 (2011).

<sup>12</sup>L. Fu, *Phys. Rev. Lett.* **103**, 266801 (2009).



- <sup>13</sup>D.-X. Qu, Y. S. Hor, J. Xiong, R. J. Cava, and N. P. Ong, *Science* **329**, 821 (2010).
- <sup>14</sup>Q. Liu, C.-X. Liu, C. Xu, X.-L. Qi, and S.-C. Zhang, *Phys. Rev. Lett.* **102**, 156603 (2009).
- <sup>15</sup>Y. L. Chen *et al.*, *Science* **329**, 659 (2010).
- <sup>16</sup>L. A. Wray *et al.*, *Nat. Phys.* **7**, 32 (2011).
- <sup>17</sup>K. Nomura and N. Nagaosa, *Phys. Rev. B* **82**, 161401(R) (2010).
- <sup>18</sup>C. J. García-Cervera and W. E. P. Schottky, *J. Appl. Phys.* **90**, 370 (2001).
- <sup>19</sup>F. S. Nogueira and I. Eremin, arXiv:1207.2731.
- <sup>20</sup>C. X. Liu, X. L. Qi, H. J. Zhang, X. Dai, Z. Fang, and S. C. Zhang, *Phys. Rev. B* **82**, 045122 (2010).
- <sup>21</sup>S. Mao, A. Yamakage, and Y. Kuramoto, *Phys. Rev. B* **84**, 115413 (2011).
- <sup>22</sup>M. Bander and D. L. Mills, *Phys. Rev. B* **38**, 12015 (1988).
- <sup>23</sup>Y. L. Chen *et al.*, *Science* **325**, 178 (2009).
- <sup>24</sup>A. P. Ramirez, *Annu. Rev. Mater. Sci.* **24**, 453 (1994).
- <sup>25</sup>S. Middelhoek, *J. Appl. Phys.* **34**, 1054 (1963).
- <sup>26</sup>P. G. Steeneken, L. H. Tjeng, I. Elfimov, G. A. Sawatzky, G. Ghiringhelli, N. B. Brookes, and D.-J. Huang, *Phys. Rev. Lett.* **88**, 047201 (2002).
- <sup>27</sup>H. Kronmüller and S. Parkin, *Handbook of Magnetism and Advanced Magnetic Materials* (Wiley, New York, USA, 2007).
- <sup>28</sup>A. Lisfi, C. M. Williams, L. T. Nguyen, J. C. Lodder, A. Coleman, H. Corcoran, A. Johnson, P. Chang, A. Kumar, and W. Morgan, *Phys. Rev. B* **76**, 054405 (2007).
- <sup>29</sup>J. E. Greedan, *J. Mater. Chem.* **11**, 37 (2001).